Wet-bulb temperature from pressure, relative humidity, and air temperature

David M. Romps[a,b]

[a] *Department of Earth and Planetary Science, University of California, Berkeley, California, USA* [b] *Climate and Ecosystem Sciences Division, Lawrence Berkeley National Laboratory, Berkeley, California, USA*

ABSTRACT: The algorithms currently in use for calculating the wet-bulb temperature from pressure, relative humidity, and air temperature have errors of a degree or more. Here, the equation for the thermodynamic wet-bulb temperature is derived using the Rankine–Kirchhoff approximations, which are highly accurate for meteorological and climatological applications. Likewise, equations are derived for the thermodynamic ice-bulb temperature and for the psychrometric wet-bulb and ice-bulb temperatures. The equations are fast to solve, requiring only a microsecond on a current laptop computer, and the results match empirical data to within hundredths of a degree. Furthermore, the equations reveal the existence of air temperatures and humidities that generate bistability: evaporating liquid water is stable at a liquid temperature above freezing and, simultaneously, sublimating ice is stable at an ice temperature below freezing.

1. Introduction

The wet-bulb temperature is used to forecast precipitation phase (e.g., Ding et al. 2014; Sims and Liu 2015), measure the relative humidity (e.g., Greenspan and Wexler 1968; ASTM International 2015), and quantify heat stress (Sherwood and Huber 2010; Vecellio et al. 2022). Unfortunately, there are many different definitions of the wet-bulb temperature (Bleeker 1939; Liljegren et al. 2008; Knox et al. 2017) and many different algorithms used to calculate the wet-bulb temperature from pressure, relative humidity, and air temperature (Martínez 1994; Davies-Jones 2008; Stull 2011; Buzan et al. 2015; Chen and Chen 2022; May et al. 2022; Raymond 2023a; Warren 2025b), and there is often ambiguity about which definition is being used or should be used. This diversity of definitions and algorithms would not pose a problem if they all gave the same answer, but, as shown here, they give values that can differ by several degrees.

Here, precise definitions will be given for the thermodynamic wet-bulb temperature, the psychrometric wet-bulb temperature, and their ice-bulb counterparts. Using the Rankine–Kirchhoff approximations (ideal gas, temperature-independent heat capacities, and zero specific volume for condensates; Romps 2021), which are highly accurate for meteorological and climatological applications (Romps 2017), we will derive equations for each of the wet-bulb and ice-bulb temperatures in terms of pressure, relative humidity, and air temperature. For more details on the Rankine–Kirchhoff approximations and the parameter values used here, see appendix A. The code to calculate these wet-bulb and ice-bulb temperatures is available as the `wetbulb` function in the `heatindex` package, available for R through CRAN and for Python through PyPI. The resulting expression for the thermodynamic wet-bulb temperature will be shown to agree with empirical data to within 0.05 K, in contrast to the existing algorithms, whose maximum errors range from 0.3 K to 2 K. Finally, we will show that the equations predict a curious bistability: there is a range of temperatures and humidities for which both a wet bulb and an ice bulb are stable.

2. Definitions

There are four different temperatures that will be defined here: thermodynamic (a.k.a., isobaric) wet-bulb, psychrometric (a.k.a., ventilated or aspirated) wet-bulb, thermodynamic ice-bulb, and psychrometric ice-bulb. In academic research, the most commonly used of these is the thermodynamic wet-bulb temperature, which is usually denoted by $T_{\rm w}$, so we retain that notation here. To denote the psychrometric wet-bulb temperature, we use $T_{\rm pw}$. Likewise, we use $T_{\rm i}$ and $T_{\rm pi}$ to denote the thermodynamic and psychrometric ice-bulb temperatures.

The air's thermodynamic wet-bulb temperature is the temperature of liquid water that does not change when subjected to isobaric thermodynamic equilibration with a parcel of the air. In other words, the thermodynamic wet-bulb temperature

Corresponding author: David M. Romps, romps@berkeley.edu

T_w is the temperature that yields the following outcome:

$$\text{parcel of liquid water } (p,T_\mathrm{w}) + \text{parcel of air } (p,T,\mathrm{RH}) \xrightarrow[\text{thermodynamic equilibration}]{} \text{parcel of liquid water } (p,T_\mathrm{w}) + \text{parcel of air } (p,T_\mathrm{w},1). \quad (1)$$

Note that the liquid water and the air parcel end up equilibrated (they are at a common temperature T_w and the air parcel is saturated), the process is isobaric (the pressure is held constant at p), and, most notably, the temperature of the liquid water does not change (its temperature remains at T_w). Note that the masses of the parcels of liquid water and air do not, in general, remain the same through this equilibration process: for RH < 1 the parcel of liquid water gives mass to the air parcel, and vice versa for RH > 1. Only for RH = 1 is there no exchange of mass, in which case $T_\mathrm{w} = T$.

Experimentally, the thermodynamic wet-bulb temperature is the temperature to which a body of liquid water asymptotes as it is repeatedly equilibrated with parcels of the air. In general, each time the liquid water is equilibrated with a new air parcel, they exchange heat and water in the process. Consider, for example, a case where the liquid water is initially at the same temperature as the air. If the air is subsaturated, then equilibration with that liquid water will evaporate some of it into the air parcel, cooling both it and the liquid to a new, lower temperature. With repeated equilibration with a sequence of air parcels, that common temperature asymptotes to the wet-bulb temperature.

The air's psychrometric wet-bulb temperature is the temperature of liquid water that does not change when subjected to an isobaric exchange of heat and moisture with a stream of the air. In other words, the psychrometric wet-bulb temperature T_pw is the temperature that yields the following outcome:

$$\text{parcel of liquid water } (p,T_\mathrm{pw}) + \text{upstream air } (p,T,\mathrm{RH}) \xrightarrow[\text{passage of air over the liquid water}]{} \text{parcel of liquid water } (p,T_\mathrm{pw}) + \text{downstream air } (p,T',\mathrm{RH}'). \quad (2)$$

As in the case of the thermodynamic wet-bulb temperature, this process is isobaric (the pressure is held constant at p) and the temperature of the liquid water does not change (its temperature remains at T_pw), but the liquid water and the stream of air do not reach equilibration (the downstream air will have a temperature T' between T and T_pw and a relative humidity RH′ between RH and 1).

In addition to wet-bulb temperatures, we can also define ice-bulb temperatures. The definitions of the thermodynamic and psychrometric ice-bulb temperatures are the same as above, but with "liquid water" replaced with "solid water" or "ice." This paper derives formulae for these four bulb temperatures and also formulae for relative humidity in terms of them.

The four wet-bulb/ice-bulb temperatures considered here are directly relevant to forecasting precipitation phase, measuring the relative humidity, and quantifying heat stress. There are, however, other definitions of the wet-bulb/ice-bulb temperatures that are not treated here. One is the natural wet-bulb or ice-bulb temperature, which is the temperature of a body of liquid water or ice that is subjected to ambient winds, plus any convection triggered by the temperature difference between the bulb and the air, plus radiation, possibly including shortwave in addition to longwave. The natural wet/ice-bulb temperature depends on the details of the setup, and so is not amenable to a general theoretical derivation. Another is the pseudo-adiabatic wet-bulb temperature (also known as the adiabatic wet-bulb temperature), which is the temperature a parcel would attain if it were 1. decompressed until its relative humidity hits unity and then 2. compressed back to its original pressure while adding liquid water (at the same instantaneous temperature as the parcel) at a rate needed to keep the parcel saturated. The wet-bulb potential temperature is the same, but compressed to a reference pressure of 1 bar. While the pseudoadiabatic wet-bulb temperature can be useful for thinking about convective motions, and the wet-bulb potential temperature can be useful for labeling saturated pseudoadiabats on thermodynamic plots, neither is particularly well-suited for the standard applications listed above. Therefore, when someone refers to the wet-bulb temperature in the context of meteorological measurements or heat stress, they are usually referring to the thermodynamic or psychrometric versions that are the topic of this paper.

Between the wet-bulb and ice-bulb temperatures, the former is much more commonly used in meteorology. And, between the thermodynamic and psychrometric wet-bulb temperatures, the phrase "wet-bulb temperature" more often refers to the former because the thermodynamic wet-bulb temperature is an unambiguous thermodynamic quantity. In contrast, the psychrometric wet-bulb temperature depends on details of thermal conductivity, mass diffusivity, and turbulence. Those effects can be approximated using the Chilton-Colburn analogy, but it must be borne in mind that

this is an approximation to real wet-bulb thermometers, the details of which will differ from one instrument to the next. Therefore, most of the results shown in section 5 will pertain to the thermodynamic wet-bulb temperature.

3. Existing algorithms

A variety of different algorithms are used to calculate the wet-bulb temperature from the air pressure, temperature, and relative humidity. These include: the expressions of Martínez (1994), Stull (2011), and Chen and Chen (2022); the implementation of the algorithm of Davies-Jones (2008) in the `HumanIndexMod` software (Buzan 2022) by Buzan et al. (2015) and in the `wetbulb_dj08_spedup2023` software (Raymond 2023b) by Raymond (2023a); and the `atmos` software (Warren 2025a) by Warren (2025b).

The most widely used equation for calculating the wet-bulb temperature comes from Stull (2011), which approximated it as a transcendental function of temperature and relative humidity. Note that this approximation does not include any dependence on total air pressure, and Stull (2011) does not state which definition of the wet-bulb temperature is being approximated. Nevertheless, this approximation for the wet-bulb temperature has been widely used to study heat stress (e.g., Lorenz et al. 2019; Saeed et al. 2021; Zhao et al. 2021; Chakraborty et al. 2022; Freychet et al. 2022; Brimicombe et al. 2023; Suarez-Gutierrez et al. 2023; Yang et al. 2023; Wang et al. 2024; Zheng et al. 2024), among other applications.

Another widely used algorithm is that of Davies-Jones (2008), which presented a method for calculating the *pseudo-adiabatic* wet-bulb temperature. Recall that the thermodynamic and psychrometric wet-bulb temperatures are the temperatures of a wetted body exposed to the ambient air, but the *pseudo-adiabatic* wet-bulb temperature is not. Therefore, the pseudo-adiabatic wet-bulb temperature is not particularly well-suited to studying the heat stress of sweat-covered humans. Nevertheless, it has been widely used in studies of heat stress (e.g., Sherwood and Huber 2010; Dunne et al. 2013; Im et al. 2017; Kang and Eltahir 2018; Coffel et al. 2018; Mishra et al. 2020; Raymond et al. 2020; Rogers et al. 2021; Schwingshackl et al. 2021; Jha et al. 2022; Simpson et al. 2023; Rockström et al. 2023; Wang et al. 2023; Vecellio et al. 2023). Here, the wet-bulb algorithm of Davies-Jones (2008) is calculated using commit 653ce06 (April 22, 2022) of the `HumanIndexMod` software (Buzan 2022) by Buzan et al. (2015) and commit 58af126 (September 27, 2023) of the `wetbulb_dj08_spedup2023` software (Raymond 2023b) by Raymond (2023a).

Less commonly used are the equations of Martínez (1994) and Chen and Chen (2022). Martínez (1994) approximated the thermodynamic wet-bulb temperature as the root of a cubic equation involving pressure, temperature, and relative humidity. Note that Martínez (1994) has two typos: a denominator in the definition of Q should be $3a^2$ instead of $3a^3$, and the last term in equation (6) should be $-b/3a$ instead of $+b/3a$. Those typos have been corrected in the implementation of the algorithm here. Chen and Chen (2022) approximates the wet-bulb temperature using a cubic polynomial in temperature and relative humidity. Note that Chen and Chen (2022) does not include a dependence on total air pressure and does not state what version of the wet-bulb temperature is being approximated.

A recent addition is the wet-bulb algorithm of Warren (2025b), which has been implemented in the `atmos` package (Warren 2025a). This algorithm uses the Rankine–Kirchhoff approximations, but its derivation contains two approximations that impair its accuracy. The first is that the liquid water to be evaporated into the air is assumed to be at the temperature of the air, not the temperature of the wet bulb; this approximation traces back to earlier works (Emanuel 1994; Ambaum 2010; Markowski and Richardson 2010). The second is the implicit assumption that the addition of liquid water to the parcel does not alter the mass fraction of water vapor. For more details, see appendix E. Here, the wet-bulb algorithm of Warren (2025b) is calculated using commit 70f58d2 (April 14, 2025) of the `atmos` package.

4. Theory

As shown in appendices B and C, the thermodynamic wet-bulb temperature T_w, psychrometric wet-bulb temperature T_pw, thermodynamic ice-bulb temperature T_i, and psychrometric ice-bulb temperature T_pi are defined implicitly in the

context of the Rankine–Kirchhoff (RK) approximations by

$$c_{\mathrm{pm}}(T-T_{\mathrm{w}}) = \frac{q_{\mathrm{v}}^{*,\mathrm{l}}(p,T_{\mathrm{w}}) - q_{\mathrm{v}}}{1-q_{\mathrm{v}}^{*,\mathrm{l}}(p,T_{\mathrm{w}})} L_{\mathrm{e}}(T_{\mathrm{w}}) \qquad \text{thermodynamic wet-bulb} \tag{3}$$

$$\mathrm{Le}^{2/3} c_{\mathrm{pm}}(T-T_{\mathrm{pw}}) = \frac{q_{\mathrm{v}}^{*,\mathrm{l}}(p,T_{\mathrm{pw}}) - q_{\mathrm{v}}}{1-q_{\mathrm{v}}^{*,\mathrm{l}}(p,T_{\mathrm{pw}})} L_{\mathrm{e}}(T_{\mathrm{pw}}) \qquad \text{psychrometric wet-bulb} \tag{4}$$

$$c_{\mathrm{pm}}(T-T_{\mathrm{i}}) = \frac{q_{\mathrm{v}}^{*,\mathrm{s}}(p,T_{\mathrm{i}}) - q_{\mathrm{v}}}{1-q_{\mathrm{v}}^{*,\mathrm{s}}(p,T_{\mathrm{i}})} L_{\mathrm{s}}(T_{\mathrm{i}}) \qquad \text{thermodynamic ice-bulb} \tag{5}$$

$$\mathrm{Le}^{2/3} c_{\mathrm{pm}}(T-T_{\mathrm{pi}}) = \frac{q_{\mathrm{v}}^{*,\mathrm{s}}(p,T_{\mathrm{pi}}) - q_{\mathrm{v}}}{1-q_{\mathrm{v}}^{*,\mathrm{s}}(p,T_{\mathrm{pi}})} L_{\mathrm{s}}(T_{\mathrm{pi}}) \qquad \text{psychrometric ice-bulb}\,. \tag{6}$$

Here, p is the total air pressure, T is the air temperature, q_{v} is the air's mass fraction of water vapor, c_{pm} is the air's specific heat capacity at constant pressure (subscript "m" for mixture or moist), L_{e} is the specific latent enthalpy of evaporation (a function of temperature, not to be confused with Le), L_{s} is the specific latent enthalpy of sublimation, $q_{\mathrm{v}}^{*,\mathrm{l}}$ is the saturation mass fraction of water vapor with respect to liquid water (assuming no condensates, this is a function only of pressure and temperature), $q_{\mathrm{v}}^{*,\mathrm{s}}$ is the saturation mass fraction of water vapor with respect to solid water (i.e., ice), and Le is the Lewis number defined as the ratio of the thermal diffusivity in air to the mass diffusivity of water vapor in air (not to be confused with L_{e}). Appendix A summarizes how c_{pm}, L_{e}, L_{s}, $q_{\mathrm{v}}^{*,\mathrm{l}}$, and $q_{\mathrm{v}}^{*,\mathrm{s}}$ are defined in the RK approximations and gives values for the thermodynamic constants used here (set to the optimal values found in Romps 2017). For meteorological applications, the Lewis number is weakly dependent on pressure, temperature, and humidity, and is within a few percent of 0.85. Here, we will take the Lewis number to be a constant equal to 0.85. Since the Lewis number is close to one, the psychrometric wet-bulb temperature is close to, but slightly less than, the thermodynamic wet-bulb temperature.

Equation (3) can be thought of as describing a two-step process for equilibrating an air parcel to a wet-bulb that is, itself, already equilibrated at the wet-bulb temperature. The first step is to cool the air parcel to the wet-bulb temperature by conducting sensible heat to the wet bulb without any phase changes. The heat transferred to the wet bulb in this process is equal to the original mass of the parcel times $c_{\mathrm{pm}}(T-T_{\mathrm{w}})$. Now that the parcel is at the same temperature as the wet bulb, we can allow evaporation of water into the parcel to saturate it. Thus, we must increase the mass fraction of water vapor in the parcel from q_{v} to $q_{\mathrm{v}}^{*,\mathrm{l}}(p,T_{\mathrm{w}})$, which is accomplished by evaporating a mass of water equal to the original mass of the parcel times $[q_{\mathrm{v}}^{*,\mathrm{l}}(p,T_{\mathrm{w}}) - q_{\mathrm{v}}]/[1-q_{\mathrm{v}}^{*,\mathrm{l}}(p,T_{\mathrm{w}})]$ (see Appendix B for a derivation). Therefore, the heat removed from the wet bulb is that mass times $L_{\mathrm{e}}(T_{\mathrm{w}})$. Since we have assumed the wet-bulb is already equilibrated at its wet-bulb temperature, its temperature cannot be changed by this process, and so the sensible heat delivered to the wet bulb must exactly equal the energy put into latent heat during evaporation. Thus, the two terms we just described — represented by the left-hand and right-hand sides of equation (3) — must be equal.

Equation (3) is an implicit equation for T_{w} in terms of p, T, and q_{v} (which shows up explicitly and also in c_{pm}). Likewise, (4), (5), and 6) are implicit equations for T_{pw}, T_{i}, and T_{pi}, respectively. Therefore, T_{w} and its analogs can be calculated from pressure, specific humidity, and air temperature using a root solver. On the other hand, if we wish to calculate the bulb temperatures from pressure, *relative humidity*, and air temperature, then we must express q_v in terms of relative humidity. Assuming no condensates in the ambient air (i.e., $q_{\mathrm{l}} = q_{\mathrm{s}} = 0$), the relative humidity with respect to liquid water $\mathrm{RH_l}$ and relative humidity with respect to solid water (ice) $\mathrm{RH_s}$ are related to q_{v} by

$$p_{\mathrm{v}} = \mathrm{RH_l} p_{\mathrm{v}}^{*,\mathrm{l}}(T) = \mathrm{RH_s} p_{\mathrm{v}}^{*,\mathrm{s}}(T) \tag{7}$$

$$q_{\mathrm{v}} = \frac{\varepsilon p_{\mathrm{v}}}{p-(1-\varepsilon)p_{\mathrm{v}}}\,, \tag{8}$$

where p_{v} is the water-vapor pressure, $p_{\mathrm{v}}^{*,\mathrm{l}}$ ($p_{\mathrm{v}}^{*,\mathrm{s}}$) is the saturation vapor pressure with respect to liquid (solid) water, $\varepsilon = R_{\mathrm{a}}/R_{\mathrm{v}}$, and R_{a} and R_{v} are the specific gas constants for dry air and water vapor, respectively. We can use these relations to obtain implicit equations for any of the bulb temperatures in terms of pressure, relative humidity, and air temperature. Furthermore, we can write those equations as *explicit* expressions for any of q_{v}, $\mathrm{RH_l}$, or $\mathrm{RH_s}$.

As shown in appendix D, the explicit expressions for $\mathrm{RH_l}$ are

$$\mathrm{RH_l} = \frac{p}{p_\mathrm{v}^{*,\mathrm{l}}(T)} \left\{ \frac{\varepsilon L_\mathrm{e}(T_\mathrm{w}) p_\mathrm{v}^{*,\mathrm{l}}(T_\mathrm{w}) - c_\mathrm{pa}(T - T_\mathrm{w}) \left[p - p_\mathrm{v}^{*,\mathrm{l}}(T_\mathrm{w}) \right]}{\varepsilon L_\mathrm{e}(T_\mathrm{w}) p + (\varepsilon c_\mathrm{pv} - c_\mathrm{pa})(T - T_\mathrm{w}) \left[p - p_\mathrm{v}^{*,\mathrm{l}}(T_\mathrm{w}) \right]} \right\} \qquad \text{in terms of } T_\mathrm{w}\,, \tag{9}$$

$$\mathrm{RH_l} = \frac{p}{p_\mathrm{v}^{*,\mathrm{l}}(T)} \left\{ \frac{\varepsilon L_\mathrm{e}(T_\mathrm{pw}) p_\mathrm{v}^{*,\mathrm{l}}(T_\mathrm{pw}) - \mathrm{Le}^{2/3} c_\mathrm{pa}(T - T_\mathrm{pw}) \left[p - p_\mathrm{v}^{*,\mathrm{l}}(T_\mathrm{pw}) \right]}{\varepsilon L_\mathrm{e}(T_\mathrm{pw}) p + \mathrm{Le}^{2/3} (\varepsilon c_\mathrm{pv} - c_\mathrm{pa})(T - T_\mathrm{pw}) \left[p - p_\mathrm{v}^{*,\mathrm{l}}(T_\mathrm{pw}) \right]} \right\} \qquad \text{in terms of } T_\mathrm{pw}\,, \tag{10}$$

$$\mathrm{RH_l} = \frac{p}{p_\mathrm{v}^{*,\mathrm{l}}(T)} \left\{ \frac{\varepsilon L_\mathrm{s}(T_\mathrm{i}) p_\mathrm{v}^{*,\mathrm{s}}(T_\mathrm{i}) - c_\mathrm{pa}(T - T_\mathrm{i}) \left[p - p_\mathrm{v}^{*,\mathrm{s}}(T_\mathrm{i}) \right]}{\varepsilon L_\mathrm{s}(T_\mathrm{i}) p + (\varepsilon c_\mathrm{pv} - c_\mathrm{pa})(T - T_\mathrm{i}) \left[p - p_\mathrm{v}^{*,\mathrm{s}}(T_\mathrm{i}) \right]} \right\} \qquad \text{in terms of } T_\mathrm{i}\text{, and} \tag{11}$$

$$\mathrm{RH_l} = \frac{p}{p_\mathrm{v}^{*,\mathrm{l}}(T)} \left\{ \frac{\varepsilon L_\mathrm{s}(T_\mathrm{pi}) p_\mathrm{v}^{*,\mathrm{s}}(T_\mathrm{pi}) - \mathrm{Le}^{2/3} c_\mathrm{pa}(T - T_\mathrm{pi}) \left[p - p_\mathrm{v}^{*,\mathrm{s}}(T_\mathrm{pi}) \right]}{\varepsilon L_\mathrm{s}(T_\mathrm{pi}) p + \mathrm{Le}^{2/3} (\varepsilon c_\mathrm{pv} - c_\mathrm{pa})(T - T_\mathrm{pi}) \left[p - p_\mathrm{v}^{*,\mathrm{s}}(T_\mathrm{pi}) \right]} \right\} \qquad \text{in terms of } T_\mathrm{pi}\,, \tag{12}$$

where c_pa (c_pv) is the specific heat capacity at constant pressure for dry air (water vapor). Note that $\mathrm{RH_s}$ can be obtained from these expressions using $\mathrm{RH_s} = \mathrm{RH_l} p_\mathrm{v}^{*,\mathrm{l}}(T) / p_\mathrm{v}^{*,\mathrm{s}}(T)$. In terms of the thermodynamic wet-bulb and ice-bulb temperatures, (9) and (11) are explicit expressions for $\mathrm{RH_l}$. Likewise, since a constant is used for the Lewis number Le, (10) and (12) are also explicit expressions for $\mathrm{RH_l}$. On the other hand, if Le were modeled as having a slight humidity dependence, then the right-hand sides of equations (10) and (12) would depend on $\mathrm{RH_l}$, and so a root solver would be needed. As indicated by the title of this manuscript, the wet-bulb temperature — or any of the other bulb temperatures — can be found from the pressure, relative humidity, and air temperature using a root solver applied to the appropriate one of equations (9–12).

In the `heatindex` package, Brent's method is used to solve the implicit equations for the bulb temperatures. On an Apple M2 chip, it takes 1 μs to calculate one wet-bulb temperature; i.e., 10^6 wet-bulb temperatures are calculated in 1 s. Since no iteration is needed to find the relative humidities from the bulb temperatures using equations (9–12), they are calculated much faster. On an Apple M2 chip, it takes 50 ns to calculate one relative humidity; i.e., 20×10^6 relative humidities are calculated in 1 s.

5. Results

Solving for T_w is done here using the optimal parameters for Rankine–Kirchhoff moist thermodynamics from Romps (2017); see Appendix A for the parameter values. To illustrate the solutions, Figure 1 plots various wet-bulb or ice-bulb temperatures minus an appropriate reference temperature. For example, the thermodynamic wet-bulb depression is $T - T_\mathrm{w}$, and the negative of this is plotted in Figure 1a for a total air pressure of 1 bar. The grey area is where the combination of temperature and relative humidity would give a vapor pressure exceeding the total air pressure, which would be unphysical. The lower limit of the temperature axis has been set to 260 K to represent a practical limit on the existence of a supercooled wet bulb.

So that the relative-humidity axis will mean the same thing in all four panels of Figure 1, the relative humidity is defined here to be $\mathrm{RH_l}$ (i.e., with respect to liquid water) for $T \geq 273.16$ K and $\mathrm{RH_s}$ (with respect to solid water) for $T < 273.16$ K. Thus, in Figure 1a, the kinks in the contours are caused by this definition of relative humidity, not by any discontinuity in the physics of wet bulbs. Also, note that $T_\mathrm{w} = T$ at $\mathrm{RH_l} = 1$ (and so $T_\mathrm{w} = T$ at the top of this panel for $T \geq 273.16$ K), but $T_\mathrm{w} \neq T$ in general at $\mathrm{RH_s} = 1$ (and so $T_\mathrm{w} \neq T$ at the top of this panel for $T < 273.16$ K).

It may seem odd to report the wet-bulb temperature at an air temperature of 400 K since that temperature is well above the boiling point of water. Note, however, the large values of the wet-bulb depression. With an air temperature of 400 K and zero relative humidity, the wet-bulb depression is an enormous 91.5 K; i.e., the wet-bulb temperature is only 308.5 K (35.4 °C or 95.7 °F). In other words, liquid water equilibrated with dry air at 1 bar and 400 K is well below its boiling point.

As mentioned in section 3, the empirical formulae of Stull (2011) and Chen and Chen (2022) have no dependence on total atmospheric pressure. As atmospheric pressure is lowered with constant T and RH, however, the wet-bulb depression increases. Figure 1b shows the difference between the thermodynamic wet-bulb temperature at 0.5 bar and the thermodynamic wet-bulb temperature at 1 bar. We see that the changes in T_w from halving the atmospheric pressure can exceed 5 K.

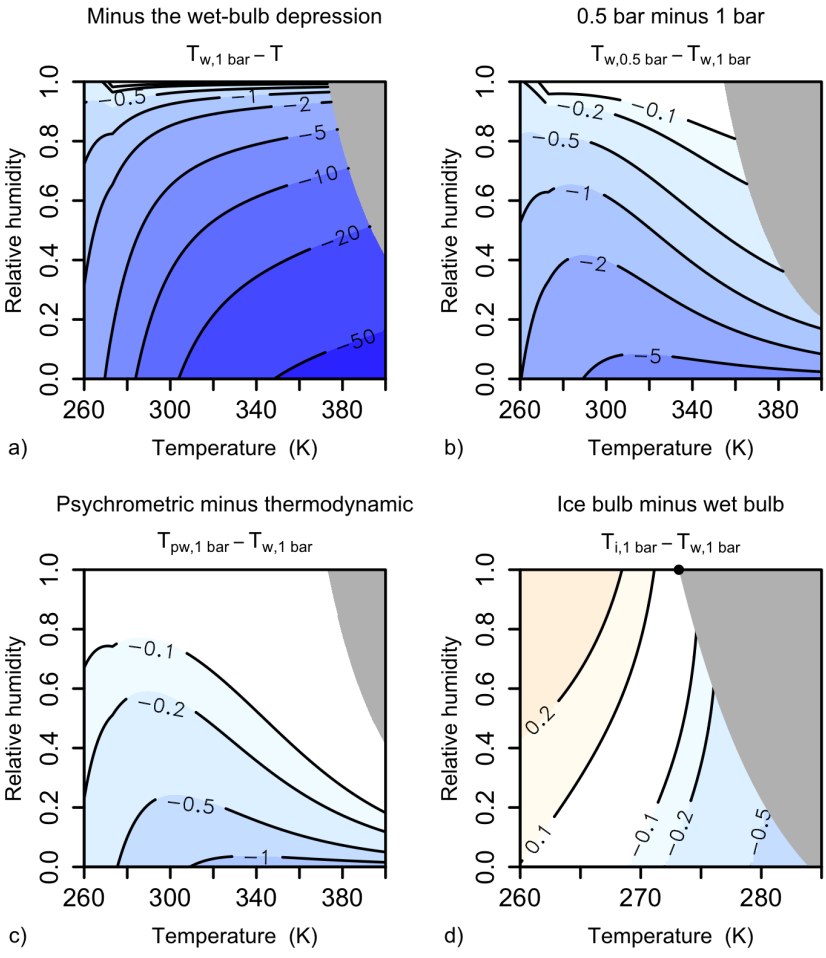

FIG. 1. (a) Minus the thermodynamic wet-bulb depression in K at an atmospheric pressure of 1 bar plotted as a function of air temperature and relative humidity. The greyed-out region is where the combination of temperature and relative humidity imply a water-vapor pressure exceeding the total atmospheric pressure of 1 bar. (b) The difference of the thermodynamic wet-bulb temperature at 0.5 bar minus the thermodynamic wet-bulb temperature at 1 bar. The greyed-out region is where water-vapor pressure would exceed 0.5 bar. (c) The difference of the psychrometric wet-bulb temperature minus the thermodynamic wet-bulb temperature at 1 bar. The greyed-out region is where water-vapor pressure would exceed 1 bar. (d) The difference of the thermodynamic ice-bulb temperature minus the thermodynamic wet-bulb temperature at 1 bar. The black circle marks where $T_w = T_i = 273.16$ K and the greyed-out region is where $T_i > 273.16$ K. Note that the range of the abscissa is different in this panel. In all of these panels, the relative humidity is defined to be RH_l for $T \geq 273.16$ K and RH_s for $T < 273.16$ K.

Figure 1c plots the difference between the psychrometric and thermodynamic wet-bulb temperatures at 1 bar. That difference grows as the relative humidity is lowered and, at zero humidity, the magnitude of the difference increases monotonically as the air temperature increases. At $T = 400$ K and RH = 0, T_{pw} is 1.6 K lower than T_w.

Figure 1d plots the difference between the ice-bulb and wet-bulb temperatures at an air pressure of 1 bar. Note that the plotted temperature range is different in this panel. A special point in this plot is $T = 273.16$ K and $RH_l = RH_s = 1$, marked by the black circle. For that temperature and relative humidity, $T_w = T_i = 273.16$ K regardless of the overall air pressure.

The grey region in panel d is where T_i is greater than 273.16 K. While such ice-bulb temperatures can be calculated, a real ice bulb is not stable at such temperatures, and so it is not a useful quantity in practice. Accordingly, that region has been greyed out. Overall, we see that the ice-bulb temperature differs from the wet-bulb temperature — where both ice is stable and super-cooled water is metastable — by less than 1 K.

For all $T > 273.16$ K, the ice-bulb temperature is lower than the wet-bulb temperature. This follows from the fact that $L_s > L_e$, which makes sublimation cooling over ice greater than evaporative cooling over liquid. On the other hand, for

Pressure (bar)	T (°C)	Observed T_w (°C)	Calculated T_w (°C)	Obs. − Calc. (°C)
0.9745	24.80	7.87	7.86	0.01
0.9737	24.73	7.81	7.82	−0.01
0.9816	24.62	7.80	7.83	−0.03
0.9806	24.65	7.82	7.84	−0.02
1.0002	25.11	8.24	8.21	0.03
0.9943	37.07	13.25	13.26	−0.01
0.9948	37.01	13.19	13.24	−0.05
0.9943	37.02	13.27	13.24	0.03
0.9978	37.02	13.23	13.28	−0.05
1.0000	24.98	8.15	8.15	0.00
1.0005	25.02	8.16	8.17	−0.01
1.0008	25.02	8.18	8.17	0.01
1.0008	25.08	8.22	8.20	0.02
1.0007	25.17	8.25	8.24	0.01

TABLE 1. (columns 1–3) Observed pressure, temperature, and thermodynamic wet-bulb temperature from the water–air experiments of Greenspan and Wexler (1968), copied from their Table 1. These are experiments in which the air has zero humidity. (column 4) The thermodynamic wet-bulb temperature calculated for these observed pressures and temperatures using equation (3) with $q_v = 0$ or, equivalently, equation (9) with $\mathrm{RH_l} = 0$. (column 5) The difference between the observed and calculated T_w.

$T < 273.16$ K, we see that there are relative humidities for which the ice-bulb temperature is *higher* than the wet-bulb temperature. This occurs because $p_v^{*,l}(T) > p_v^{*,s}(T)$ for $T < 273.16$ K. To see the connection, consider a point on the top edge of panel d to the left of the circle, i.e., $\mathrm{RH_s} = 1$ and $T < 273.16$ K. There, T_i equals T, but a wet bulb feels subsaturated conditions ($\mathrm{RH_l} < 1$) and so will evaporate into the air, leading to $T_w < T_i$.

6. Evaluating the algorithms

To evaluate the accuracy of equations (3) and (9), we can compare against Greenspan and Wexler (1968), which measured the thermodynamic wet-bulb temperature for air with zero humidity. Here, we take all of their water–air measurements except that, following Greenspan and Wexler (1968), we reject the experiments performed at the high flow rate of 6.2 liters per minute. The observed values of p, T, and T_w from Greenspan and Wexler (1968) are given in the first three columns of Table 1. The fourth column contains T_w calculated from (3) or, equivalently, (9) using the observed p and T and $q_v = \mathrm{RH_l} = 0$.

The maximum absolute error of the differences between observed and calculated T_w (column 5 of Table 1) is 0.05 K. The histogram of these errors is shown in the top row of Figure 2. We see that the errors are centered on zero, exhibiting no obvious bias. Furthermore, the standard deviation of these errors of 0.03 K closely matches the estimated random error in the measurements of 0.02 K (Greenspan and Wexler 1968). This suggests that the small spread in the distribution of differences is likely due either largely or predominantly to observational measurement error.

If we repeat this evaluation for the other algorithms, we get the other six rows of Figure 2. We see that none of the other distributions of errors are centered on zero. Compared to the maximum error of 0.05 K for equation (3), the maximum errors for the other algorithms are substantially larger: 0.3 K for Martínez (1994), 0.3 K for Stull (2011), 1.2 K for Buzan et al. (2015), 1.9 K for Chen and Chen (2022), 1.2 K for Raymond (2023a), and 0.4 K for Warren (2025b).

To give these errors further context, the six panels of Figure 3 plot the difference between T_w calculated with the six other algorithms minus the T_w calculated with equation (3). For $T \in [260, 400]$ K and $\mathrm{RH} \in [0, 1]$, we see that all of the other algorithms deviate by as much as 1 K or more. For Martínez (1994), Stull (2011), and Chen and Chen (2022), the deviations can exceed 10 K. For Buzan et al. (2015) and Raymond (2023a) — both based on Davies-Jones (2008) — there are large regions in which the algorithms do not converge. Of the prior algorithms, that of Warren (2025b), which also uses the Rankine–Kirchhoff approximations, comes the closest to the correct values, but substantial deviations remain due to other approximations in the associated derivation, as discussed in Appendix E.

In practice, either of the equivalent equations (3) or (9) should be used to solve for the thermodynamic wet-bulb temperature T_w in place of the other existing algorithms. This recommendation is based on the following: 1. equation (3) is grounded in the highly accurate Rankine–Kirchhoff approximations (Romps 2021, 2017), 2. solutions to equation (3) match the available empirical data for the thermodynamic wet-bulb temperature (Table 1 and Figure 2), and 3. solving equation (3) has a low computational cost of only 1 μs on a standard laptop (using the `wetbulb` function in the `heatindex` package). Since equations (4), (5), and (6) are likewise grounded in the same Rankine–Kirchhoff approximations, they are recommended for calculating the psychrometric wet-bulb, thermodynamic ice-bulb, and psychrometric ice-bulb,

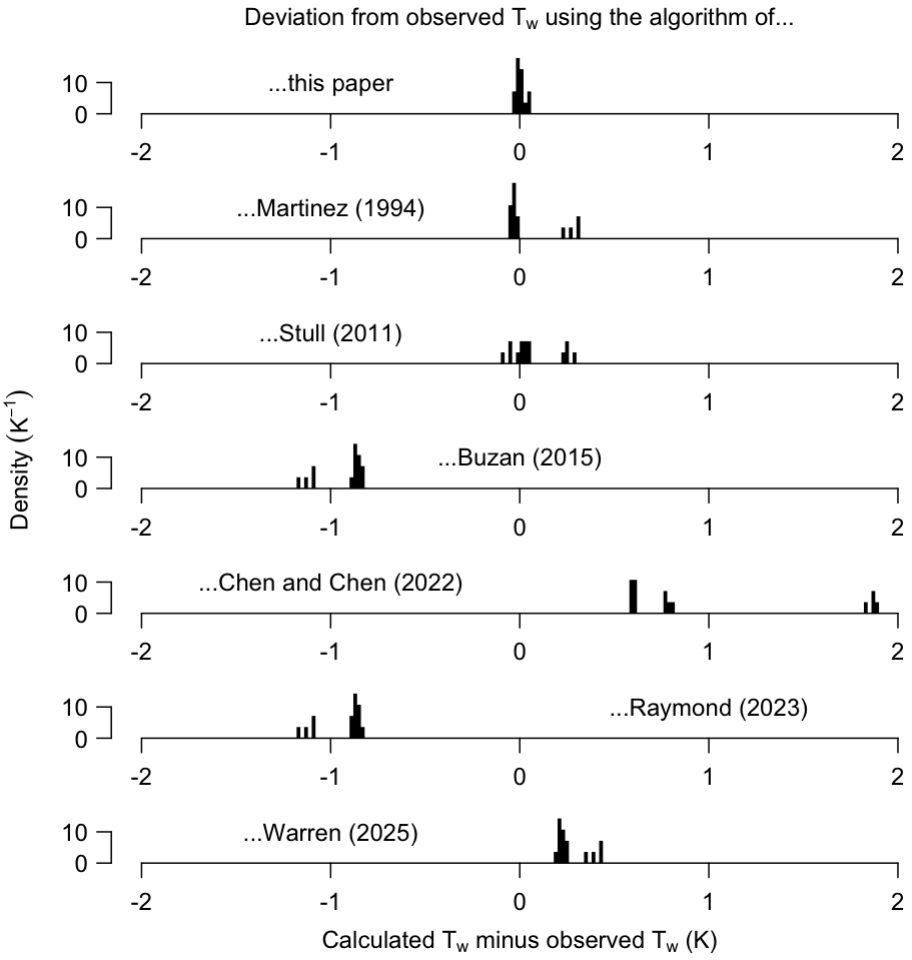

FIG. 2. Error, in K, relative to the empirical thermodynamic wet-bulb temperatures measured by Greenspan and Wexler (1968) for (row 1) equation (3) of this paper, (row 2) the expression of Martínez (1994), (row 3) the expression of Stull (2011), (row 4) the implementation of Davies-Jones (2008) in the `HumanIndexMod` software of Buzan et al. (2015), (row 5) the expression of Chen and Chen (2022), (row 6) the implementation of Davies-Jones (2008) in the `wetbulb_dj08_spedup2023` software of Raymond (2023a), and (row 7) the `atmos` software of Warren (2025b).

respectively. All four of these bulb temperatures can be calculated using the `wetbulb` function in the `heatindex` package.

7. Bistability of water and ice

To explore the aforementioned bistability, let us revisit Figure 1d. Recall that the black circle is where T_w and T_i both equal the triple-point temperaure of 273.16 K (0.01 °C). In the Rankine–Kirchhoff approximations, condensates are incompressible, so the melting point equals this triple-point temperature independent of atmospheric pressure. Therefore, directly to the right of the black circle in Figure 1d, and also anywhere in the grey region, an ice bulb is unstable because $T_i > 273.16$ K and so it would spontaneously melt. The left edge of the grey region in Figure 1d is the curve where $T_i = 273.16$ K, i.e., where a thermodynamic ice bulb is at its melting point.

An interesting observation is that the ice-bulb depression is greater than the wet-bulb depression along this ice-bulb melting-point curve, as can be seen by the warm colors there in Figure 1d. This means that $T_i < T_w$. Therefore, for RH < 1, there is a region just to the left of the grey curve in which $T_i < 273.16$ K and $T_w > 273.16$ K. In other words, there is a sliver of temperature–humidity space where both an ice bulb and a wet bulb are simultaneously stable.

It is important to emphasize here the difference between stability and metastability. Farther to the left of the grey region in Figure 1d, e.g., at $T = 270$ K, a wet bulb can be in a supercooled metastable state. But if we were to briefly

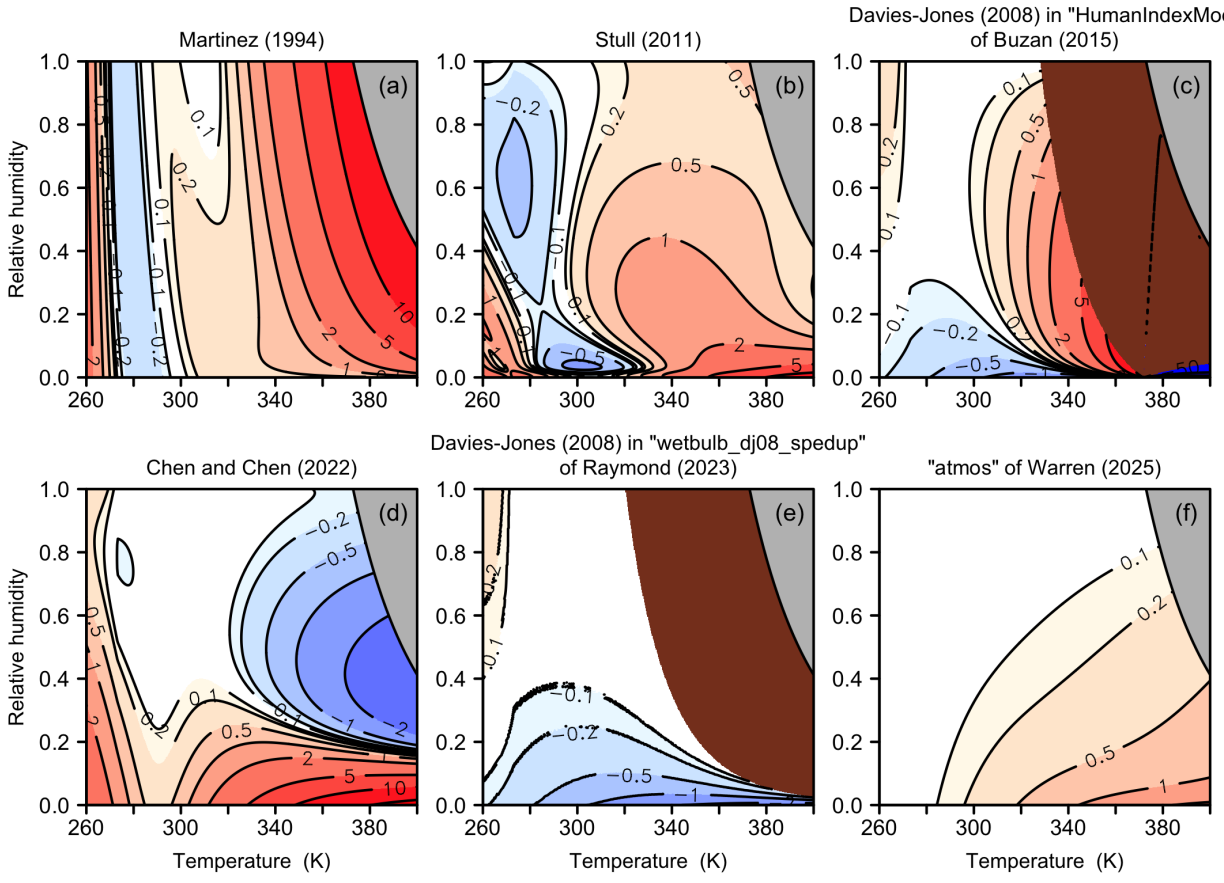

FIG. 3. (a) Difference, in kelvin, of T_w from the algorithm of Martínez (1994) minus the exact Rankine–Kirchhoff T_w from equation (3) at 1 bar of total atmospheric pressure. (b) Same, but for Stull (2011) versus equation (3). (c) Same, but for Davies-Jones (2008) as implemented by Buzan et al. (2015) versus equation (3). (d) Same, but for Chen and Chen (2022) versus equation (3). (e) Same, but for Davies-Jones (2008) as implemented by Raymond (2023a) versus equation (3). (f) Same, but for Warren (2025b) versus equation (3). In all panels, the grey region is where the combination of temperature and relative humidity imply a water-vapor pressure exceeding the total atmospheric pressure of 1 bar, and the brown regions are where the algorithms give either no value or a value that is erroneous by more than 50 K.

touch that wet bulb to an ice bulb, the wet bulb would nucleate ice and rapidly freeze over. In contrast, the small sliver of temperature–humidity space to the left of the greyed-out region is where an ice bulb and a wet bulb are both *stable*. In other words, we could briefly touch the ice bulb to the wet bulb with no substantial consequences: the ice bulb would remain frozen at a temperature below 273.16 K and the wet bulb would remain liquid at a temperature above 273.16 K.

Figure 4a shows, in yellow, the location of the sliver of temperature–humidity space where a thermodynamic ice bulb and a thermodynamic wet bulb are both stable. As expected, the sliver collapses to zero width at RH = 1, i.e., the location of the small black circle. The sliver is widest at RH = 0. Figure 4b plots T_w and T_i as a function of air temperature with RH = 0 and p = 1 bar. At this humidity and pressure, it is predicted that an air temperature between 9.5 and 10.8 °C will support both a thermodynamic ice bulb and a thermodynamic wet bulb. For a psychrometric wet bulb and a psychrometric ice bulb (not plotted), bistability is predicted to occur for RH = 0 and p = 1 bar for air temperatures in the range of 10.6 to 12.0 °C. As the air pressure decreases, an ice bulb remains stable up to even higher temperatures, and the range of temperatures yielding a bistability widens. Although of little relevance to Earth's atmosphere, it is amusing to note that, at RH = 0 and p = 0.1 bar, thermodynamic ice bulbs and wet bulbs are both predicted to be stable for air temperatures between 100.8 and 114.3 °C.

Acknowledgments. This work was supported by the U.S. Department of Energy, Office of Science, Office of Biological and Environmental Research, under Award Number DE-SC0025214. Thanks are due to Yi-Chuan Lu for feedback on

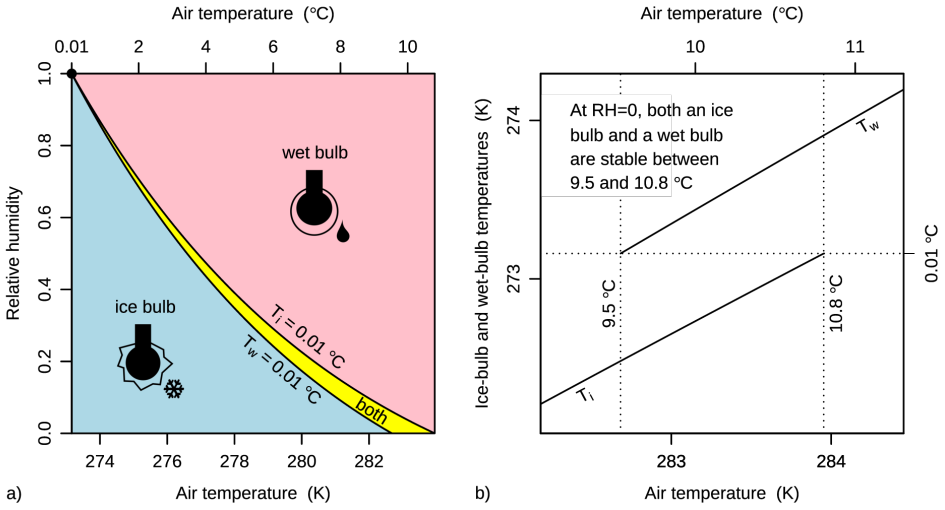

FIG. 4. (a) Regions of temperature–humidity space where only the thermodynamic ice bulb is stable (blue), where only the thermodynamic wet bulb is stable (pink), and where both are stable (yellow), calculated at a pressure of 1 bar. In the yellow region, the thermodynamic wet bulb has a temperature above 273.16 K (0.01 °C) and the thermodynamic ice bulb has a temperature below 273.16 K (0.01 °C). (b) At zero humidity and 1 bar, T_i and T_w as functions of temperature. Between 282.7 K (9.5 °C) and 284.0 K (10.8 °C), the thermodynamic ice bulb and thermodynamic wet bulb are both stable.

the manuscript and for agreeing to host the `wetbulb` function in the `heatindex` package; to Robert Warren for providing feedback on the manuscript that led to several improvements; and to two anonymous reviewers.

Data availability statement. The source code for computing the wet-bulb and ice-bulb temperatures using equations (3–6) is publicly available as part of the `heatindex` package at `https://github.com/davidromps/heatindex`. The software is also distributed as packages for R and Python, available from CRAN (`https://cran.r-project.org/web/packages/heatindex`) and PyPI (`https://pypi.org/project/heatindex`), respectively. Documentation and usage examples can be found on the `heatindex` homepage at `https://heatindex.org`. Commit 653ce06 (April 22, 2022) of the `HumanIndexMod` software is available at `https://github.com/jrbuzan/HumanIndexMod_2020/tree/653ce06400e6334737f854ebfa8a4930db678255` and at `https://archive.softwareheritage.org/browse/revision/653ce06400e6334737f854ebfa8a4930db678255`. Commit 58af126 (September 27, 2023) of the `wetbulb_dj08_spedup2023` software is available at `https://github.com/cr2630git/wetbulb_dj08_spedup/tree/58af1265e2bb25acbe9be57e53b8fbd784b915ee` and at `https://archive.softwareheritage.org/browse/revision/58af1265e2bb25acbe9be57e53b8fbd784b915ee`. Commit 70f58d2 (April 14, 2025) of the `atmos` software is available at `https://github.com/robwarrenwx/atmos/tree/70f58d2b28e204a96a82bbb7e834bfc2aab486ba` and at `https://archive.softwareheritage.org/browse/revision/70f58d2b28e204a96a82bbb7e834bfc2aab486ba`.

APPENDIX A

Rankine–Kirchhoff approximations

In the Rankine–Kirchhoff (RK) approximations, we model dry air and water vapor as ideal gases, model heat capacities as independent of temperature, and set the specific volumes of condensed water (liquid and ice) to zero (Romps 2021). The RK approximations lead to analytic equations for moist thermodynamics that are highly accurate for meteorological and climatological applications (Romps 2017). For a parcel of air with no condensates, the ideal-gas law allows us to write

$$p = (1 - q_v) R_a \rho T + q_v R_v \rho T, \tag{A1}$$

where p, ρ, T, and q_v are the air's pressure, density, temperature, and mass fraction of water vapor, respectively, and R_a and R_v are the specific gas constants for dry air and water vapor, respectively. This can also be written as $p = R_m \rho T$,

Constant	Value	Definition
R_a	287.04 J kg^{-1} K^{-1}	specific gas constant of dry air
R_v	461.4 J kg^{-1} K^{-1}	specific gas constant of water vapor
c_{vv}	1418 J kg^{-1} K^{-1}	specific heat capacity of water vapor at constant volume
c_{vl}	4216 J kg^{-1} K^{-1}	specific heat capacity of liquid water at constant volume
c_{vs}	2106 J kg^{-1} K^{-1}	specific heat capacity of solid water at constant volume
c_{pa}	1006.04 J kg^{-1} K^{-1}	specific heat capacity of dry air at constant pressure
c_{pv}	$c_{vv} + R_v$	specific heat capacity of water vapor at constant pressure
E_{0v}	2374000 J kg^{-1}	difference in specific internal energy between vapor and liquid at the triple point
E_{0s}	333700 J kg^{-1}	difference in specific internal energy between liquid and solid at the triple point
p_{trip}	611.65 Pa	triple-point pressure of water
T_{trip}	273.16 K	triple-point temperature of water
Le	0.85	Lewis number for moist air

TABLE A 1. Thermodynamic constants tuned by Romps (2017) to optimize the agreement between the RK expression for saturation vapor pressure and empirical data, plus the value used for the Lewis number.

where $R_m = (1-q_v)R_a + q_v R_v$ is the specific heat capacity of moist air with no condensates[1]. Likewise, in the absence of condensates, the specific heat capacity of moist air at constant pressure is $c_{pm} = (1-q_v)c_{pa} + q_v c_{pv}$, where c_{pa} and c_{pv} are the specific heat capacities at constant pressure of dry air and water vapor, respectively[2]. The temperature independence of heat capacities and the zero specific volumes of condensates allow us to write the latent heat of evaporation L_e and the latent heat of sublimation L_s as

$$L_e = E_{0v} + R_v T + (c_{vv} - c_{vl})(T - T_{trip}) \tag{A2}$$

$$L_s = E_{0v} + E_{0s} + R_v T + (c_{vv} - c_{vs})(T - T_{trip}), \tag{A3}$$

where c_{vv}, c_{vl}, and c_{vs} are the specific heat capacities at constant volume for vapor, liquid, and solid, E_{0v} is the difference in specific internal energy between water vapor and liquid water at the triple-point temperature T_{trip}, and E_{0s} is the difference in specific internal energy between liquid water and solid water at the triple-point temperature T_{trip}. The saturation vapor pressures with respect to liquid water $p_v^{*,l}$ and with respect to solid water $p_v^{*,s}$ are

$$\begin{aligned} p_v^{*,l} &= p_{trip}\left(\frac{T}{T_{trip}}\right)^{(c_{pv}-c_{vl})/R_v} \exp\left[\frac{L_e(T_{trip})}{R_v T_{trip}} - \frac{L_e(T)}{R_v T}\right] \\ p_v^{*,s} &= p_{trip}\left(\frac{T}{T_{trip}}\right)^{(c_{pv}-c_{vs})/R_v} \exp\left[\frac{L_s(T_{trip})}{R_v T_{trip}} - \frac{L_s(T)}{R_v T}\right], \end{aligned} \tag{A4}$$

where p_{trip} is the triple-point pressure. Assuming no condensates, equation (8) allows us to write $q_v^{*,l}$ and $q_v^{*,s}$ in terms of these saturation vapor pressures as

$$q_v^{*,l} = \frac{\varepsilon p_v^{*,l}}{p - (1-\varepsilon)p_v^{*,l}} \tag{A5}$$

$$q_v^{*,s} = \frac{\varepsilon p_v^{*,s}}{p - (1-\varepsilon)p_v^{*,s}}, \tag{A6}$$

where $\varepsilon = R_a/R_v$. Table 7 gives the values of the thermodynamic parameters used here.

APPENDIX B

Derivation of thermodynamic wet-bulb temperature

[1]If the mass fractions of liquid and solid water, q_l and q_s, are potentially non-zero, then we must write the pressure as $p = (1 - q_v - q_l - q_s)R_a\rho T + q_v R_v \rho T$ and the expression for R_m as $R_m = (1 - q_v - q_l - q_s)R_a + q_v R_v$. In the definition of the wet-bulb and ice-bulb temperatures, the parcel or stream of air is in contact with liquid or solid water at its boundary, but the air never has liquid or solid water inside it, so $q_l = q_s = 0$.

[2]If the mass fractions of liquid and solid water, q_l and q_s, are non-zero, this expression for c_{pm} generalizes to $c_{pm} = (1 - q_v - q_l - q_s)c_{pa} + q_v c_{pa} + q_l c_{vl} + q_s c_{vs}$. Here, c_{vl} and c_{vs} are the heat capacities at constant volume for liquid and solid water, which are equal to their corresponding heat capacities at constant pressure because the condensates are assumed to have zero specific volume and, thus, are incompressible.

To derive the thermodynamic wet-bulb temperature, let us refer to the ambient air as being in state 1, and let us denote the temperature, dry-air mass, and water-vapor mass of an air parcel in state 1 as T_1, M_a, and M_v1, respectively. Let T_2, M_a, and M_v2 be the air parcel's values in state 2, which is after the parcel has equilibrated with the wet bulb. Let us assume that the temperature of the wet bulb is equal to the thermodynamic wet-bulb temperature (as would be achieved practically by exposure to a large sequence of air parcels initially in state 1). Therefore, the temperature of the wet bulb both before and after contact with the air parcel must be T_2. Let M_l1 and M_l2 be the masses of liquid water on the wet bulb in states 1 and 2, respectively.

We may define the specific internal energies using any additive constant we want so long as we are consistent across the phases of water. For simplicity, we may define dry air as having zero internal energy at absolute zero, in which case its specific internal energy is $c_\mathrm{va}T$, where c_va is the specific heat capacity of dry air at constant volume. For the phases of water, we may choose the triple-point temperature T_trip as the temperature at which liquid water has zero internal energy. The specific internal energy of liquid water is then $c_\mathrm{vl}(T - T_\mathrm{trip})$. Defining E_0v (E_0s) to be the difference in specific internal energy between vapor and liquid (between liquid and solid) at the triple point, the specific internal energy of water vapor is $c_\mathrm{vv}(T - T_\mathrm{trip}) + E_\mathrm{0v}$ and that of solid water is $c_\mathrm{vs}(T - T_\mathrm{trip}) - E_\mathrm{0s}$. In the Rankine–Kirchhoff approximations, only dry air and water vapor have nonzero specific volumes, so the specific enthalpies of liquid and solid water are the same as their specific internal energies, while the specific enthalpies of dry air and water vapor are $c_\mathrm{va}T + R_\mathrm{a}T = c_\mathrm{pa}T$ and $c_\mathrm{vv}(T - T_\mathrm{trip}) + E_\mathrm{0v} + R_\mathrm{v}T$, respectively.

Therefore, the enthalpy (of air parcel and wet bulb) in state 1 is

$$M_\mathrm{a}c_\mathrm{pa}T_1 + M_\mathrm{v1}\Big[c_\mathrm{vv}(T_1 - T_\mathrm{trip}) + E_\mathrm{0v} + R_\mathrm{v}T_1\Big] + M_\mathrm{l1}c_\mathrm{vl}(T_2 - T_\mathrm{trip})\,. \tag{B1}$$

The enthalpy (of air parcel and wet bulb) in state 2 is

$$M_\mathrm{a}c_\mathrm{pa}T_2 + M_\mathrm{v2}\Big[c_\mathrm{vv}(T_2 - T_\mathrm{trip}) + E_\mathrm{0v} + R_\mathrm{v}T_2\Big] + M_\mathrm{l2}c_\mathrm{vl}(T_2 - T_\mathrm{trip})\,. \tag{B2}$$

The difference in these enthalpies must be zero for this adiabatic process at constant pressure, so, equating these two and using $c_\mathrm{pv} = c_\mathrm{vv} + R_\mathrm{v}$, we get

$$0 = (M_\mathrm{a}c_\mathrm{pa} + M_\mathrm{v1}c_\mathrm{pv})(T_2 - T_1) + (M_\mathrm{v2} - M_\mathrm{v1})\Big[c_\mathrm{vv}(T_2 - T_\mathrm{trip}) + E_\mathrm{0v} + R_\mathrm{v}T_2\Big] + (M_\mathrm{l2} - M_\mathrm{l1})c_\mathrm{vl}(T_2 - T_\mathrm{trip})\,. \tag{B3}$$

Since the total mass of water (vapor plus liquid) is unchanged, we have $M_\mathrm{v1} + M_\mathrm{l1} = M_\mathrm{v2} + M_\mathrm{l2}$, so we can replace $M_\mathrm{l2} - M_\mathrm{l1}$ with $M_\mathrm{v1} - M_\mathrm{v2}$, which allows us to write the enthalpy difference as

$$0 = (M_\mathrm{a}c_\mathrm{pa} + M_\mathrm{v1}c_\mathrm{pv})(T_2 - T_1) + (M_\mathrm{v2} - M_\mathrm{v1})L_\mathrm{e}(T_2)\,, \tag{B4}$$

where

$$L_\mathrm{e}(T) = \Big[(c_\mathrm{vv} - c_\mathrm{vl})(T - T_\mathrm{trip}) + E_\mathrm{0v} + R_\mathrm{v}T\Big] \tag{B5}$$

is the latent enthalpy of evaporation.

Dividing equation (B4) by $M_\mathrm{a} + M_\mathrm{v1}$, moving the sensible-heat term to the left-hand side, and using the definition of the air's mass fractions,

$$q_\mathrm{a1} = \frac{M_\mathrm{a}}{M_\mathrm{a} + M_\mathrm{v1}} \tag{B6}$$

$$q_\mathrm{v1} = \frac{M_\mathrm{v1}}{M_\mathrm{a} + M_\mathrm{v1}} \tag{B7}$$

$$q_\mathrm{a2} = \frac{M_\mathrm{a}}{M_\mathrm{a} + M_\mathrm{v2}} \tag{B8}$$

$$q_\mathrm{v2} = \frac{M_\mathrm{v2}}{M_\mathrm{a} + M_\mathrm{v2}}\,, \tag{B9}$$

we get

$$(q_\mathrm{a1}c_\mathrm{pa} + q_\mathrm{v1}c_\mathrm{pv})(T_1 - T_2) = \frac{M_\mathrm{v2} - M_\mathrm{v1}}{M_\mathrm{a} + M_\mathrm{v1}}L_\mathrm{e}(T_2)\,. \tag{B10}$$

Note that $(M_{v2} - M_{v1})/(M_a + M_{v1})$ is the mass of water added to the air parcel per original mass of the air parcel, which we can write as

$$\begin{aligned}
\frac{M_{v2} - M_{v1}}{M_a + M_{v1}} &= \frac{M_{v2}}{M_a + M_{v1}} - \frac{M_{v1}}{M_a + M_{v1}} \\
&= \frac{M_{v2}}{M_a + M_{v2}} \frac{M_a + M_{v2}}{M_a} \frac{M_a}{M_a + M_{v1}} - \frac{M_{v1}}{M_a + M_{v1}} \\
&= q_{v2} \frac{q_{a1}}{q_{a2}} - q_{v1} \\
&= q_{v2} \frac{1 - q_{v1}}{1 - q_{v2}} - q_{v1} \\
&= \frac{q_{v2}(1 - q_{v1})}{1 - q_{v2}} - \frac{q_{v1}(1 - q_{v2})}{1 - q_{v2}} \\
&= \frac{q_{v2} - q_{v1}}{1 - q_{v2}} \,.
\end{aligned} \tag{B11}$$

Therefore, we have

$$(q_{a1} c_{pa} + q_{v1} c_{pv})(T_1 - T_2) = \frac{q_{v2} - q_{v1}}{1 - q_{v2}} L_e(T_2) \,. \tag{B12}$$

Noting that $q_{a1} c_{pa} + q_{v1} c_{pv} = c_{pm}$ (the moist heat capacity at constant pressure of the ambient air), $T_1 = T$ (the ambient air temperature), $T_2 = T_w$ (the thermodynamic wet-bulb temperature), $q_{v1} = q_v$ (the specific humidity of the ambient air), and $q_{v2} = q_v^{*,l}(p, T_w)$, we can write this as equation (3). The equation for T_i can be derived in the same way, but with $q_v^{*,s}$ instead of $q_v^{*,l}$ and L_s instead of L_e, yielding equation (5).

APPENDIX C

Derivation of psychrometric wet-bulb temperature

To derive the psychrometric wet-bulb temperature, consider a point on the surface of the wet bulb and the molar fluxes of water vapor and dry air perpendicular to that surface. Let us define the gas's reference frame there as the frame in which the outward molar flux of water vapor j_v and the outward molar flux of dry air j_a are purely diffusive (as opposed to diffusive plus advective) and are equal and opposite, i.e., $j_a = -j_v$. Importantly, the mass transfer coefficient k based on mole fraction (dimensions of mol m^{-2} s^{-1}) is defined in terms of that *gas-relative* flux j_v according to

$$j_v = k\left[x_{vb} - x_v\right], \tag{C1}$$

where x_{vb} is the molar fraction of water vapor at the surface of the bulb and x_v is the molar fraction of water vapor in the upstream ambient air.

Since j_v is the flux of water vapor in the gas's reference frame, it is not the flux of water vapor in the wet bulb's reference frame. To derive that flux, let us use n_b, n_{vb}, and n_{ab} to denote the total, water-vapor, and dry-air molar concentrations at the bulb's surface, with $n_{ab} + n_{vb} = n_b$. Since the flux of dry air must be zero at the bulb's surface in the bulb's reference frame, the gas's reference frame must be moving away from the bulb's surface at a speed u such that $n_{ab} u + j_a = 0$. This tells us that the gas's reference frame moves outward at a speed $u = -j_a/n_{ab} = j_v/n_{ab}$. Therefore, in the bulb's reference frame, the outward molar flux of water vapor is not j_v, but is

$$n_{vb} u + j_v = n_{vb} \frac{j_v}{n_{ab}} + j_v = \frac{n_b}{n_{ab}} j_v = \frac{1}{x_{ab}} j_v = \frac{j_v}{1 - x_{vb}} \,, \tag{C2}$$

where $x_{ab} = n_{ab}/n_b = 1 - x_{vb}$ is the molar fraction of dry air at the surface of the bulb. Noting that x_{vb} equals $x_v^{*,l}(p, T_{pw})$, which is the saturation molar fraction with respect to liquid at pressure p and temperature T_{pw}, and using equation (C1) to replace j_v, we find that the flux of water vapor away from the wet bulb in the wet bulb's frame is

$$k \frac{x_v^{*,l}(p, T_{pw}) - x_v}{1 - x_v^{*,l}(p, T_{pw})} \,. \tag{C3}$$

The outward flux of latent enthalpy equals this outward molar flux of water vapor times the molar mass of water vapor m_v and the specific latent enthalpy of evaporation $L_\mathrm{e}(T_\mathrm{pw})$. Meanwhile, that outward flux of latent enthalpy must, in a steady state, equal the inward flux of sensible heat, which is equal to $h(T - T_\mathrm{pw})$, where h is the heat transfer coefficient (dimensions of W m^{-2} K^{-1}). Therefore, we have

$$h(T - T_\mathrm{pw}) = k \frac{x_\mathrm{v}^{*,\mathrm{l}}(p, T_\mathrm{pw}) - x_\mathrm{v}}{1 - x_\mathrm{v}^{*,\mathrm{l}}(p, T_\mathrm{pw})} m_\mathrm{v} L_\mathrm{e}(T_\mathrm{pw}) \,. \tag{C4}$$

Using the Chilton–Colburn analogy, we know that h and k are approximately related by

$$h = k c_\mathrm{pm} m_\mathrm{m} \mathrm{Le}^{2/3} \,, \tag{C5}$$

where c_pm is the specific heat capacity at constant pressure for the ambient moist air, m_m is the molar mass of the ambient moist air, and $\mathrm{Le} = \mathrm{Sc}/\mathrm{Pr} = \alpha/D$, where Sc is the Schmidt number, Pr is the Prandtl number, α is the thermal diffusivity, and D is the mass diffusivity. Using this to replace h in (C4), the factors of k cancel, giving us

$$\mathrm{Le}^{2/3} c_\mathrm{pm} m_\mathrm{m} (T - T_\mathrm{pw}) = \frac{x_\mathrm{v}^{*,\mathrm{l}}(p, T_\mathrm{pw}) - x_\mathrm{v}}{1 - x_\mathrm{v}^{*,\mathrm{l}}(p, T_\mathrm{pw})} m_\mathrm{v} L_\mathrm{e}(T_\mathrm{pw}) \,. \tag{C6}$$

Dividing by m_m and noting that $m_\mathrm{v}/m_\mathrm{m} = R_\mathrm{m}/R_\mathrm{v}$, and also multiplying the right-hand side by p/p, we get

$$\mathrm{Le}^{2/3} c_\mathrm{pm} (T - T_\mathrm{pw}) = L_\mathrm{e}(T_\mathrm{pw}) \frac{R_\mathrm{m}}{R_\mathrm{v}} \frac{p_\mathrm{v}^{*,\mathrm{l}}(T_\mathrm{pw}) - p_\mathrm{v}}{p - p_\mathrm{v}^{*,\mathrm{l}}(T_\mathrm{pw})} \,. \tag{C7}$$

Now, consider two different parcels of moist air (with no condensates), which we label as 1 and 2, that have the same total pressure p. We may note that

$$\begin{aligned}
\frac{p_\mathrm{v1} - p_\mathrm{v2}}{p - p_\mathrm{v1}} &= \frac{\frac{R_\mathrm{v} q_\mathrm{v1}}{R_\mathrm{m1}} p - \frac{R_\mathrm{v} q_\mathrm{v2}}{R_\mathrm{m2}} p}{p - \frac{R_\mathrm{v} q_\mathrm{v1}}{R_\mathrm{m1}} p} \\
&= R_\mathrm{v} \frac{R_\mathrm{m2} q_\mathrm{v1} - R_\mathrm{m1} q_\mathrm{v2}}{R_\mathrm{m1} R_\mathrm{m2} - R_\mathrm{v} R_\mathrm{m2} q_\mathrm{v1}} \\
&= \frac{R_\mathrm{v}}{R_\mathrm{m2}} \frac{\left[(1 - q_\mathrm{v2}) R_\mathrm{a} + q_\mathrm{v2} R_\mathrm{v}\right] q_\mathrm{v1} - \left[(1 - q_\mathrm{v1}) R_\mathrm{a} + q_\mathrm{v1} R_\mathrm{v}\right] q_\mathrm{v2}}{\left[(1 - q_\mathrm{v1}) R_\mathrm{a} + q_\mathrm{v1} R_\mathrm{v}\right] - R_\mathrm{v} q_\mathrm{v1}} \\
&= \frac{R_\mathrm{v}}{R_\mathrm{m2}} \frac{q_\mathrm{v1} - q_\mathrm{v2}}{1 - q_\mathrm{v1}} \,.
\end{aligned} \tag{C8}$$

Using this fact, equation (C7) can be written as equation (4). The equation for T_pi can be derived in the same way, but with $q_\mathrm{v}^{*,\mathrm{s}}$ instead of $q_\mathrm{v}^{*,\mathrm{l}}$ and L_s instead of L_e, yielding equation (6).

APPENDIX D

Relative humidity from wet-bulb temperature

If we want to get relative humidity from the dry-bulb temperature T and the thermodynamic wet-bulb temperature T_w, we can start from equation (3), which we write here as

$$0 = c_\mathrm{pm}(T_\mathrm{w} - T) + \frac{q_\mathrm{v}^{*,\mathrm{l}}(p, T_\mathrm{w}) - q_\mathrm{v}}{1 - q_\mathrm{v}^{*,\mathrm{l}}(p, T_\mathrm{w})} L_\mathrm{e}(T_\mathrm{w}) \,. \tag{D1}$$

To make the dependence on q_v explicit, we can write (D1) as

$$0 = c_\mathrm{pa}(T_\mathrm{w} - T) + q_\mathrm{v}(c_\mathrm{pv} - c_\mathrm{pa})(T_\mathrm{w} - T) + \frac{q_\mathrm{v}^{*,\mathrm{l}}(p, T_\mathrm{w}) - q_\mathrm{v}}{1 - q_\mathrm{v}^{*,\mathrm{l}}(p, T_\mathrm{w})} L_\mathrm{e}(T_\mathrm{w}) \tag{D2}$$

$$= c_\mathrm{pa}(T_\mathrm{w} - T) + \frac{q_\mathrm{v}^{*,\mathrm{l}}(p, T_\mathrm{w})}{1 - q_\mathrm{v}^{*,\mathrm{l}}(p, T_\mathrm{w})} L_\mathrm{e}(T_\mathrm{w}) + \left[(c_\mathrm{pv} - c_\mathrm{pa})(T_\mathrm{w} - T) - \frac{L_\mathrm{e}(T_\mathrm{w})}{1 - q_\mathrm{v}^{*,\mathrm{l}}(p, T_\mathrm{w})} \right] q_\mathrm{v} \,. \tag{D3}$$

Note that this equation is linear in q_v. Using equation (8), q_v can be written as

$$q_\mathrm{v} = \frac{\varepsilon \mathrm{RH_l} p_\mathrm{v}^{*,\mathrm{l}}(T)}{p - (1 - \varepsilon)\mathrm{RH_l} p_\mathrm{v}^{*,\mathrm{l}}(T)} \,. \tag{D4}$$

We can use (D4) to replace q_v in (D3), obtaining

$$0 = \left[c_\mathrm{pa}(T_\mathrm{w} - T) + \frac{q_\mathrm{v}^{*,\mathrm{l}}(p, T_\mathrm{w})}{1 - q_\mathrm{v}^{*,\mathrm{l}}(p, T_\mathrm{w})} L_\mathrm{e}(T_\mathrm{w}) \right] \left[p - (1 - \varepsilon)\mathrm{RH_l} p_\mathrm{v}^{*,\mathrm{l}}(T) \right] + \left[(c_\mathrm{pv} - c_\mathrm{pa})(T_\mathrm{w} - T) - \frac{L_\mathrm{e}(T_\mathrm{w})}{1 - q_\mathrm{v}^{*,\mathrm{l}}(p, T_\mathrm{w})} \right] \varepsilon \mathrm{RH_l} p_\mathrm{v}^{*,\mathrm{l}}(T) \,. \tag{D5}$$

Since (D5) is linear in $\mathrm{RH_l}$, it is straightforward to solve for $\mathrm{RH_l}$. This same procedure can be replicated for the psychrometric wet-bulb temperature and the ice-bulb temperatures, yielding equations (9–12).

APPENDIX E

Approximations in the wet-bulb algorithm of Warren (2025b)

There are two unnecessary approximations in the implementation of the wet-bulb algorithm in the `atmos` package (commit 70f58d2 on April 14, 2025) of Warren (2025b). That algorithm is based on the following equation,

$$c_\mathrm{pm}^*(p, \tilde{T}_\mathrm{w})(T - \tilde{T}_\mathrm{w}) = \left[q_\mathrm{v}^{*,\mathrm{l}}(p, \tilde{T}_\mathrm{w}) - q_\mathrm{v}' \right] L_\mathrm{e}(T) \,, \tag{E1}$$

where $c_\mathrm{pm}^*(p, \tilde{T}_\mathrm{w})$ is the specific heat capacity at constant pressure for a saturated parcel of air with no condensates at pressure p and temperature $\tilde{T}_\mathrm{w}$, and the meaning of $\tilde{T}_\mathrm{w}$ and q_v' will be explained below. Equation (E1) differs markedly from equation (3), which, replicated here for ease of comparison, is

$$c_\mathrm{pm}(T - T_\mathrm{w}) = \frac{q_\mathrm{v}^{*,\mathrm{l}}(p, T_\mathrm{w}) - q_\mathrm{v}}{1 - q_\mathrm{v}^{*,\mathrm{l}}(p, T_\mathrm{w})} L_\mathrm{e}(T_\mathrm{w}) \,. \tag{3}$$

Note that, in equation (3), c_pm is the specific heat capacity at constant pressure for the ambient moist air. The differences between equations (E1) and (3) are caused by the first approximation in Warren (2025b), which is the assumption that the liquid to be evaporated starts at the temperature of the parcel T, not at the temperature of the wet bulb T_w. This approximation traces back to earlier works (Emanuel 1994; Ambaum 2010; Markowski and Richardson 2010). As a result, the q_v' in (E1) is not the water-vapor mass fraction of the ambient air. Instead, q_v' is the water-vapor mass fraction after just enough liquid water, at temperature T, has been added to the ambient air such that, when evaporated, the air will be brought to saturation at temperature $\tilde{T}_\mathrm{w}$. Despite the fact that $q_\mathrm{v}' \neq q_\mathrm{v}$, the wet-bulb algorithm in the `atmos` software treats them as equal, which is the second approximation.

We can rewrite (E1) in terms of the actual water-vapor mass fraction q_v of the ambient air (i.e., before any liquid water is added) as follows. Note that

$$q_\mathrm{v} = M_\mathrm{v} / (M_\mathrm{a} + M_\mathrm{v}) \tag{E2}$$

$$q_\mathrm{l} = 0 \,, \tag{E3}$$

where M_a and M_v are the masses of dry air and water vapor in the parcel of ambient air. After a mass of liquid water M_l is added, the parcel then has a water-vapor mass fraction q'_v and liquid-water mass fraction q'_l given by

$$q'_\mathrm{v} = M_\mathrm{v}/(M_\mathrm{a} + M_\mathrm{v} + M_\mathrm{l}) \tag{E4}$$
$$q'_\mathrm{l} = M_\mathrm{l}/(M_\mathrm{a} + M_\mathrm{v} + M_\mathrm{l})\,. \tag{E5}$$

Therefore,

$$\begin{aligned} 1/q'_\mathrm{v} &= (M_\mathrm{a} + M_\mathrm{v} + M_\mathrm{l})/M_\mathrm{v} \\ &= (M_\mathrm{a} + M_\mathrm{v})/M_\mathrm{v} + M_\mathrm{l}/M_\mathrm{v} \\ &= 1/q_\mathrm{v} + q'_\mathrm{l}/q'_\mathrm{v}\,. \end{aligned} \tag{E6}$$

In other words, $q_\mathrm{v} = q'_\mathrm{v}/(1 - q'_\mathrm{l})$. Since M_l is the amount of water that must be added such that $q'_\mathrm{v} + q'_\mathrm{l} = q_\mathrm{v}^{*,\mathrm{l}}(p, \tilde{T}_\mathrm{w})$, we can use this fact to eliminate q'_l from this relation to obtain

$$q'_\mathrm{v} = \frac{1 - q_\mathrm{v}^{*,\mathrm{l}}(p, \tilde{T}_\mathrm{w})}{1 - q_\mathrm{v}}\, q_\mathrm{v}\,. \tag{E7}$$

Therefore, equation (E1) from Warren (2025b) can be written as

$$c^*_\mathrm{pm}(p, \tilde{T}_\mathrm{w})(T - \tilde{T}_\mathrm{w}) = \frac{q_\mathrm{v}^{*,\mathrm{l}}(p, \tilde{T}_\mathrm{w}) - q_\mathrm{v}}{1 - q_\mathrm{v}}\, L_\mathrm{e}(T)\,. \tag{E8}$$

This bears some resemblance to equation (3), but it is not the same. Furthermore, the $\tilde{T}_\mathrm{w}$ that solves equation (E8) is not the wet-bulb temperature T_w.

References

Ambaum, M. H. P., 2010: *Thermal Physics of the Atmosphere*. Wiley-Blackwell.

ASTM International, 2015: E337-15. ASTM E337–15: Standard Test Method for Measuring Humidity with a Psychrometer (the Measurement of Wet- and Dry-Bulb Temperatures). ASTM, West Conshohocken, PA, URL https://doi.org/10.1520/E0337-15, Annual Book of ASTM Standards, https://doi.org/10.1520/E0337-15.

Bleeker, W., 1939: On the conservatism of the equivalent potential and the wet-bulb potential temperatures. *Quarterly Journal of the Royal Meteorological Society*, **65 (282)**, 542–550.

Brimicombe, C., C. H. B. Lo, F. Pappenberger, C. Di Napoli, P. Maciel, T. Quintino, R. Cornforth, and H. L. Cloke, 2023: Wet Bulb Globe Temperature: Indicating extreme heat risk on a global grid. *GeoHealth*, **7 (2)**, e2022GH000 701.

Buzan, J. R., 2022: HumanIndexMod. GitHub, commit 653ce06 (2022-04-22), https://github.com/jrbuzan/HumanIndexMod_2020.

Buzan, J. R., K. Oleson, and M. Huber, 2015: Implementation and comparison of a suite of heat stress metrics within the Community Land Model version 4.5. *Geoscientific Model Development*, **8 (2)**, 151–170.

Chakraborty, T., Z. S. Venter, Y. Qian, and X. Lee, 2022: Lower urban humidity moderates outdoor heat stress. *AGU Advances*, **3 (5)**, e2022AV000 729.

Chen, H.-Y., and C.-C. Chen, 2022: An empirical equation for wet-bulb temperature using air temperature and relative humidity. *Atmosphere*, **13 (11)**, 1765, https://doi.org/10.3390/atmos13111765, URL https://doi.org/10.3390/atmos13111765.

Coffel, E. D., R. M. Horton, and A. de Sherbinin, 2018: Temperature and humidity based projections of a rapid rise in global heat stress exposure during the 21st century. *Environmental Research Letters*, **13 (1)**, 014 001.

Davies-Jones, R., 2008: An efficient and accurate method for computing the wet-bulb temperature along pseudoadiabats. *Monthly Weather Review*, **136 (7)**, 2764–2785.

Ding, B., K. Yang, J. Qin, L. Wang, Y. Chen, and X. He, 2014: The dependence of precipitation types on surface elevation and meteorological conditions and its parameterization. *Journal of Hydrology*, **513**, 154–163.

Dunne, J. P., R. J. Stouffer, and J. G. John, 2013: Reductions in labour capacity from heat stress under climate warming. *Nature Climate Change*, **3 (6)**, 563–566.

Emanuel, K. A., 1994: *Atmospheric Convection*. Oxford University Press, USA.

Freychet, N., G. C. Hegerl, N. S. Lord, Y. E. Lo, D. Mitchell, and M. Collins, 2022: Robust increase in population exposure to heat stress with increasing global warming. *Environmental Research Letters*, **17 (6)**, 064 049.

Greenspan, L., and A. Wexler, 1968: An adiabatic saturation psychrometer. *Journal of Research of the National Bureau of Standards – C. Engineering and Instrumentation*, **72C (1)**, 33–47.

Im, E.-S., J. S. Pal, and E. A. B. Eltahir, 2017: Deadly heat waves projected in the densely populated agricultural regions of South Asia. *Science Advances*, **3 (8)**, e1603 322.

Jha, R., A. Mondal, A. Devanand, M. K. Roxy, and S. Ghosh, 2022: Limited influence of irrigation on pre-monsoon heat stress in the Indo-Gangetic Plain. *Nature Communications*, **13 (1)**, 4275.

Kang, S., and E. A. B. Eltahir, 2018: North China Plain threatened by deadly heatwaves due to climate change and irrigation. *Nature Communications*, **9 (1)**, 2894.

Knox, J. A., D. S. Nevius, and P. N. Knox, 2017: Two simple and accurate approximations for wet-bulb temperature in moist conditions, with forecasting applications. *Bulletin of the American Meteorological Society*, **98 (9)**, 1897–1906.

Liljegren, J. C., R. A. Carhart, P. Lawday, S. Tschopp, and R. Sharp, 2008: Modeling the wet bulb globe temperature using standard meteorological measurements. *Journal of Occupational and Environmental Hygiene*, **5 (10)**, 645–655.

Lorenz, R., Z. Stalhandske, and E. M. Fischer, 2019: Detection of a climate change signal in extreme heat, heat stress, and cold in Europe from observations. *Geophysical Research Letters*, **46 (14)**, 8363–8374.

Markowski, P., and Y. Richardson, 2010: *Mesoscale Meteorology in Midlatitudes*. John Wiley & Sons.

Martínez, A. T., 1994: On the evaluation of the wet bulb temperature as a function of dry bulb temperature and relative humidity. *Atmósfera*, **7 (3)**.

May, R. M., and Coauthors, 2022: MetPy: A meteorological Python library for data analysis and visualization. *Bulletin of the American Meteorological Society*, **103 (10)**, E2273–E2284.

Mishra, V., A. K. Ambika, A. Asoka, S. Aadhar, J. Buzan, R. Kumar, and M. Huber, 2020: Moist heat stress extremes in India enhanced by irrigation. *Nature Geoscience*, **13 (11)**, 722–728.

Raymond, C., 2023a: Davies-Jones revisited. Regional Climate Perspectives, blog post, https://www.regionalclimateperspectives.com/blog/archives/09-2023.

Raymond, C., 2023b: wetbulb_dj08_spedup: Numba-optimized Python implementation of the Davies-Jones 2008 wet-bulb-temperature algorithm. GitHub, commit 58af126 (2023-09-27), https://github.com/cr2630git/wetbulb_dj08_spedup.

Raymond, C., T. Matthews, and R. M. Horton, 2020: The emergence of heat and humidity too severe for human tolerance. *Science Advances*, **6 (19)**, eaaw1838.

Rockström, J., and Coauthors, 2023: Safe and just Earth system boundaries. *Nature*, **619 (7968)**, 102–111.

Rogers, C. D. W., M. Ting, C. Li, K. Kornhuber, E. D. Coffel, R. M. Horton, C. Raymond, and D. Singh, 2021: Recent increases in exposure to extreme humid-heat events disproportionately affect populated regions. *Geophysical Research Letters*, **48 (19)**, e2021GL094 183.

Romps, D. M., 2017: Exact expression for the lifting condensation level. *Journal of the Atmospheric Sciences*, **74 (12)**, 3891–3900.

Romps, D. M., 2021: The Rankine-Kirchhoff approximations for moist thermodynamics. *Quarterly Journal of the Royal Meteorological Society*, **147 (740)**, 3493–3497.

Saeed, F., C.-F. Schleussner, and M. Ashfaq, 2021: Deadly heat stress to become commonplace across South Asia already at 1.5°C of global warming. *Geophysical Research Letters*, **48 (7)**, e2020GL091 191.

Schwingshackl, C., J. Sillmann, A. M. Vicedo-Cabrera, M. Sandstad, and K. Aunan, 2021: Heat stress indicators in CMIP6: Estimating future trends and exceedances of impact-relevant thresholds. *Earth's Future*, **9 (3)**, e2020EF001 885.

Sherwood, S. C., and M. Huber, 2010: An adaptability limit to climate change due to heat stress. *Proceedings of the National Academy of Sciences*, **107 (21)**, 9552–9555.

Simpson, C. H., O. Brousse, K. L. Ebi, and C. Heaviside, 2023: Commonly used indices disagree about the effect of moisture on heat stress. *NPJ Climate and Atmospheric Science*, **6 (1)**, 78.

Sims, E. M., and G. Liu, 2015: A parameterization of the probability of snow–rain transition. *Journal of Hydrometeorology*, **16 (4)**, 1466–1477.

Stull, R., 2011: Wet-bulb temperature from relative humidity and air temperature. *Journal of Applied Meteorology and Climatology*, **50 (11)**, 2267–2269.

Suarez-Gutierrez, L., W. A. Müller, and J. Marotzke, 2023: Extreme heat and drought typical of an end-of-century climate could occur over Europe soon and repeatedly. *Communications Earth & Environment*, **4 (1)**, 415.

Vecellio, D. J., Q. Kong, W. L. Kenney, and M. Huber, 2023: Greatly enhanced risk to humans as a consequence of empirically determined lower moist heat stress tolerance. *Proceedings of the National Academy of Sciences*, **120 (42)**, e2305427 120, https://doi.org/10.1073/pnas.2305427120, URL https://doi.org/10.1073/pnas.2305427120.

Vecellio, D. J., S. T. Wolf, R. M. Cottle, and W. L. Kenney, 2022: Evaluating the 35 °C wetbulb temperature adaptability threshold for young, healthy subjects (PSU HEAT Project). *Journal of Applied Physiology*, **132 (2)**, 340–345.

Wang, F., M. Gao, C. Liu, R. Zhao, and M. B. McElroy, 2024: Uniformly elevated future heat stress in China driven by spatially heterogeneous water vapor changes. *Nature Communications*, **15 (1)**, 4522.

Wang, P., Y. Yang, D. Xue, L. Ren, J. Tang, L. R. Leung, and H. Liao, 2023: Aerosols overtake greenhouse gases causing a warmer climate and more weather extremes toward carbon neutrality. *Nature Communications*, **14 (1)**, 7257.

Warren, R., 2025a: atmos: fast and accurate calculations for applications in atmospheric science. GitHub, commit 70f58d2 (2025-04-14), https://github.com/robwarrenwx/atmos.

Warren, R. A., 2025b: A consistent treatment of mixed-phase saturation for atmospheric thermodynamics. *Quarterly Journal of the Royal Meteorological Society*, **151 (766)**, e4866.

Yang, J., L. Zhao, and K. Oleson, 2023: Large humidity effects on urban heat exposure and cooling challenges under climate change. *Environmental Research Letters*, **18 (4)**, 044 024.

Zhao, L., and Coauthors, 2021: Global multi-model projections of local urban climates. *Nature Climate Change*, **11 (2)**, 152–157.

Zheng, Z., X. Lin, L. Chen, C. Yan, and T. Sun, 2024: Effects of urbanization and topography on thermal comfort during a heat wave event: A case study of Fuzhou, China. *Sustainable Cities and Society*, **102**, 105 233.